

# **A MECHANISTIC STUDY OF FIRE RETARDANCY OF CARBON NANOTUBE/EVA AND THEIR CLAY COMPOSITES**

**Fengge Gao and Qingchun Yuan**

School of Biomedical and Natural Sciences, Nottingham Trent University, Clifton Lane,  
Nottingham, NG11 8NS, UK

**Gunter Beyer**

Kabelwerk Eupen AG, Malmedyerstrasse 9  
B-4700 Eupen, Belgium

## **Corresponding Author**

Dr. Fengge Gao  
School of Biomedical and Natural Sciences  
Nottingham Trent University  
Clifton Lane  
Nottingham  
NG11 8NS  
UK

Email: [fengge.gao@ntu.ac.uk](mailto:fengge.gao@ntu.ac.uk)

Tel: +44 115 848 6042  
Fax: +44 115 848 6506

# A MECHANISTIC STUDY OF FIRE RETARDANCY OF CARBON NANOTUBE/EVA AND THEIR CLAY COMPOSITES

Fengge Gao\*<sup>1</sup>, Gunter Beyer<sup>2</sup>, Qingchun Yuan<sup>1</sup>

<sup>1</sup>School of Biomedical and Natural Sciences, Nottingham Trent University, Clifton Lane, Nottingham, NG11 8NS, UK

<sup>2</sup>Kabelwerk Eupen AG, Malmedyerstrasse 9  
B-4700 Eupen, Belgium

\*Corresponding Author: Fengge Gao, Email: fengge.gao@ntu.ac.uk, Tel: +44 115 848 6042, Fax: +44 115 848 6506

## Abstract

A further investigation of the roles of multi-walled carbon nanotubes and clay in the fire retardancy of EVA nanocomposites has been carried out. It was found that the nanotubes played an important role in the reduction of the peak of heat release rate by forming low permeable char containing graphitic carbon. The oxidation resistance of the char is a function of the degree of graphitisation. Adding clay into the nanotube/EVA composite tends to enhance the formation of graphitic carbon. The nanotubes also have the function to reduce surface cracks of chars to increase barrier resistance to the evolution of flammable volatiles and the oxygen ingress to the condensed phase.

**Keywords:** Carbon nanotubes; clay; fire retardant; nanocomposites; ethylene-vinyl acetate

## Introduction

Since the discovery of carbon nanotubes by Iijima a decade ago<sup>1</sup>, significant progress has been made in the development of this new class of material. Currently, both single and multi-walled carbon nanotubes can be produced commercially in small-scale. This rapid progress in nanotube fabrication has stimulated the application of carbon nanotubes in the enhancement of a wide range of engineering properties<sup>2-7</sup>. One of these interests is fire retardancy. Beyer initiated this activity two years ago<sup>8</sup>. Since then, the team at the NIST, University of Kentucky and Nottingham Trent University have joined the force to progress the work in this field further. So far three journal

papers relevant to fire retardancy of carbon nanotube enhanced polymers have been published<sup>8-10</sup>. These investigations provided preliminary evaluation and understanding of the effect of adding a small amount of multi-walled carbon nanotubes (MWNT) in ethylene-vinyl acetate (EVA) and polypropylenes (PP) on the peak of heat release rate of the MWNT/polymer composites in cone calorimeter test. For both polymer systems, the peak of heat release rate was reduced by introducing multi-walled carbon nanotubes. In the latest publication, the influences of the nanotube concentration in polypropylene, the iron particles in the nanotubes and the thermal conductivity of fillers on flammability of MWNT/PP composites were also investigated<sup>[10]</sup>.

This paper will report the further progress of our previous work on carbon nanotube enhanced EVA composites. In the previous study, three types of EVA composite containing MWNT, organoclay and the mixture of clay and MWNT were investigated via cone calorimeter test **as shown in Fig 1**<sup>8</sup>. The results indicated that carbon nanotubes were more effective in reducing the rate of heat release rate than the organoclay. However in the residual char structure produced by the combustion, an integrated structure with surface cracks was formed from the clay/EVA nanocomposites while only limited char fragments were obtained in the composite containing the nanotubes. These structures does not appear to support the results on the peak of heat release rate if the fire retardant action of the nanotubes occurs in the condensed phase as indicated in the latest publication on MWNT/PP composites<sup>10</sup>. If the nanotubes could not lead to the formation of sufficient char in the condensed phase, the polymer at the condensed phase could not be well protected. Therefore it would be expected that the peak of the heat release rate of MWNT/EVA composite should be higher than that of the clay/EVA composite. In order to understand this, further investigation of these materials have been carried out under different burning conditions using x-ray diffraction analysis (XRD) and scanning electron microscopy (SEM).

## **Experimental**

The three composite systems investigated were EVA enhanced with 5phr (part per hundred) multi-wall carbon nantubes, organoclays and the mixture of nanotube and clay respectively. They are

named as MWNT/EVA composite, clay/EVA nanocomposite and clay/MWNT/EVA nanocomposite correspondingly. In the clay/MWNT/EVA nanocomposite, the weight ratio between MWNT and clay was 1:1, i.e., the composite containing 2.5phr MWNT and 2.5phr clay.

The EVA copolymer used had commercially name Escorene 00328 supplied by Exxon. The polymer contained 28wt% vinyl acetate. The multi-walled nanotube applied comprised 99wt% MWNT and 1wt% minerals. The major mineral components, measured using atomic absorption spectrometry, were Fe, Al<sub>2</sub>O<sub>3</sub> and Co. The product was supplied by the University of Namur, Belgium. The MWNT/EVA composites were produced by melt extrusion of pre-blended mixture of nanotube/EVA using a Brabender at 130°C.

In the clay/EVA and clay/MWNT/EVA nanocomposites, the organoclay used was a montmorillonite modified by N,N-dimethyl-N,N-dioctadecylammonium cations. The same processing condition as applied to the nanotube composite was used to produce clay/EAV and clay/MWNT/EVA nanocomposites.

Flammability of the composites was characterised using cone calorimeter test under 35 kW/m<sup>2</sup> heat flux. Three tests for each material were conducted. The deviation of the data between the three tests was found to be within ±5% for all the materials studied. The composites were also burnt by applying a natural burning test and furnace-burning test at 600°C for 20 minutes in a Muffle furnace to introduce different extent of char oxidation during combustion. In the natural burning test, plate shaped samples with dimension 30 mm x 30 mm x 3 mm were burnt using a Bunsen burner under a well-ventilated condition. The length of the flame of the burner was controlled to 6mm. The colour of the flame was adjusted by changing air flowing rate of the burner, progressively from orange to just blue. The blue flame was used to ignite a sample at 45° angle to the flat surface of the sample for 1 min. Following ignition, the flame was removed. The sample was burnt naturally. The char structure produced in different combustion processes was studied using scanning electron microscopy. The nano-structure of the composites and chars was

characterised using x-ray diffraction analysis by applying Cr as the radiation source with wavelength,  $\lambda = 0.229$  nm.

## Results and Discussion

Fig. 2 shows the morphology of the chars of the composites produced by the cone calorimeter test and the natural burning experiment respectively. The chars produced from clay/EVA nanocomposite had a similar structure in both tests. Significant difference can be observed in the MWNT/EVA and clay/MWNT/EVA composites in the two burning conditions. Most of the char of MWNT/EVA composite was burnt out in the cone calorimeter test whilst an integrated char structure with relative smooth surface was formed in the natural burning experiment. For the composite containing both nanotubes and clay, the cone calorimeter test resulted in a well-formed char with smooth surface. A very different structure was formed in the natural burning test. The morphology of the char in this case is similar to the appearance of the char produced from the clay/EVA nanocomposite. However the extent of surface cracks has been reduced.

The natural burning process can be considered as a milder combustion with less extent of char oxidation compared to the cone calorimeter test. This process may be representative to the early stage of the combustion in the cone calorimeter test. Compared to the clay/EVA nanocomposite, the char with smooth surface and a very limited few cracks formed from the MWNT/EVA composite in the early stage of combustion may be responsible for the larger extent of reduction of the peak of heat release rate. Such a structure has better barrier resistance to the evolution of flammable volatiles to the vapour phase and the oxygen ingress to the condensed phase than the highly cracked char structure in the clay/EVA system. However the oxidation resistance of the char formed from the nanotube-enhanced composite may not be as good as the char formed from the clay/EVA nanocomposite. In this case, if the samples are exposed long time to a constant heat flux as occurring in the cone calorimeter test, higher reactive char formed in the nanotube composite would be burnt out, leading to the formation of the structure of the char as shown in the top row in Fig.2.

If this explanation were correct, the small plate samples with size 30 mm x 30 mm x 3 mm should result in the similar char structure to what was observed in the cone calorimeter test if an extensive oxidation condition were applied. In order to achieve this, the samples were burnt in a Muffle furnace at 600°C for 20 minutes. The morphology of the chars formed in this process is shown in Fig.3. It can be observed that the nanotube enhanced EVA was almost burnt out while an integrated char structure was retained in the clay/EVA nanocomposite. This proves the validity of the speculation and shows that the chars formed from different resources exhibit different reactivity to oxidation.

For the composite containing both clay and carbon nanotubes (clay/MWTN/EVA), similar char morphology was obtained in both natural burning and Muffle furnace tests. The chars formed had an integrated structure with moderate surface cracks. This structure is significantly different from the smooth char structure of the same composite obtained in the cone calorimeter test. At present, it has not yet been understood the causes of this difference.

The mechanism of char oxidation was explored using x-ray diffractometry. The samples for XRD analysis were produced by burning the samples in a Muffle furnace at 600°C for 4 minutes. In such a period of time, significant amount of chars can be obtained from all samples for the XRD investigation. Fig. 4 shows the XRD patterns of the composites before and after burning under this condition. For the clay/EVA nanocomposite, the (001) peak of the clay at 3.87nm can be seen clearly in the XRD pattern of the sample before burning. Following the combustion, this peak has been shifted to a wider angle beyond 4.5nm. It is understood from these data that the original composite has an intercalated structure. Some species may remain between the clay layers following the burning. Two new peaks appear at 0.3337nm and 0.3172nm in the XRD pattern of the char. These peaks are close to the (002) peak of graphite. However they are unlikely to be associated with graphitic carbon since the interlayer distance is smaller than that of pure graphite, 0.3354nm. It is well known in the carbon community that the interlayer spacing of chars formed from organic species during carbonisation should be larger than the interlayer spacing of pure

graphite<sup>11-13</sup>. During carbonisation and graphitisation processes, aromatic layers are formed first in the organic species and are stacked together progressively to form ordered polycrystalline carbons. The interlayer spacing decreases correspondingly from infinitive large for amorphous structure via a transition value for detectable ordered 3-D crystallites 0.344nm in turbostratic carbons towards the graphitic value 0.3354nm for the perfect graphite structure. Therefore the two peaks in the (002) region of the clay/EVA nanocomposites should not be associated with the formation of turbostratic and graphitic carbon structures. The fringe in the (100, 101) region close to  $66^\circ$  gives additional support to this analysis. The characteristic (100, 101) peaks of turbostratic and graphitic carbons are not visible in this region.

The results obtained from this study make the picture of the char structure of clay/polymer nanocomposites more blur. In the early study of clay/polymer nanocomposites, the NIST group considered that the char formed by clay/polymer nanocomposites was essentially silicate sheets containing voids<sup>14</sup>. In their latest investigation on clay/nylon-6 nanocomposites, two peaks at 0.335nm and 0.325nm have been identified in the XRD pattern of the char of the composites<sup>15</sup>. In their analysis, both peaks were considered as the (002) peaks of graphitic carbon. This should be re-considered according to the results obtained in this study and the analysis described in the previous paragraph. At present, a better understanding of the char structure of clay/polymer nanocomposites is a key issue towards understanding the mechanism of fire retardancy. We are currently in the progress to investigate this further.

For the nanotube-enhanced composite, the sample before burning does not have a graphitic structure. An intensive broad peak appears at 0.3445nm in the XRD pattern of the char. This is the characteristic feature of turbostratic carbon so that turbostratic carbon structure has been formed during the combustion of MWNT/EVA composite. In such a structure, a number of aromatic layers stacked together roughly parallel and equidistant, but with each layer having completely random orientation about the layer normal.

In the case of the composite containing both nanotube and clay, perfect crystallites of graphite can be identified. A broad peak at 0.3354nm is visible in the XRD pattern of the char. This is exactly the interlayer distance of pure graphite. However pure graphite has very sharp (002) peak. The broaden peak may indicate that the stacking height of the crystallites is small. The char may contain a mixture of graphite crystallites, turbostratic carbons and graphitic carbon. The degree of graphitisation is higher than that of the nanotube enhanced composite without clay.

For both MWNT/EVA and clay/MWNT/EVA composites, the (100, 101) peaks are clearly visible in the corresponding XRD patterns of the chars. This confirms the formation of turbostratic and graphitic carbons in these materials during combustion.

It appears from the results obtained that the oxidation resistance of char is a function of carbon structure of the chars and the presence of clay. Although turbostratic carbon has been formed during the combustion of the nanotube enhanced composite, the lower degree of graphitisation in the char has relatively high reactivity to oxidation leading to the char burnt out in the long time exposure to a high extent of heat flux as occurring in the core calorimeter test and Muffle furnace burning at 600°C for 20 minutes. Our experiment on pure graphite shows that pure graphite did not suffer significant weight loss in such combustion conditions. Therefore a higher degree of graphitisation in the char structure tends to give better protection to char from oxidation.

Adding clay in the nanotube enhanced EVA could promote the formation of graphitic structure and increase the resistance of char oxidation. The reason may be associated with that silicates themselves cannot be burnt. At this stage of investigation, it is not yet clear the reason for the catalytic effect of clay on graphitisation.

The difference in the surface cracking between the char samples was investigated using SEM on the fractured surface of chars. The fractured surfaces were created by bending the chars using hands. The SEM micrographs of the fractured surfaces of two char samples produced from clay/EVA and MWNT/EVA using the same combustion condition as applied to the XRD samples are shown in Fig.5 a and b respectively. The fractured surfaces were suited in the areas pointed by



white arrows. The fracture surface of the char of clay/EVA nanocomposite appears clean while the pulled out nanotubes can be identified on the fractured surface of the char produced from the nanotube-enhanced composite. This indicates that the nanotubes play an important role in preventing crack formation. The fibrous nanotubes tend to bind the matrix together to reduce the extent of surface cracking during combustion leading to the formation of smoothed char surface in the early stage of combustion.

## **Conclusion**

This study provides a further understanding of the roles of multi-walled carbon nanotubes and clay in fire retardancy of EVA composites. Nanotubes may act as the nucleation of graphitisation leading to the formation of turbostratic and graphitic carbons. This effect has been enhanced when both nanotubes and clay are applied. The formation of graphitic carbon in char may contribute directly to the reduction of the peak of heat release rate of the composites. The nanotubes also have the function to reduce surface cracks of chars, leading to the increase of barrier resistance to the evolution of flammable volatiles and the oxygen ingress to the condensed phase.

The research also demonstrates that char oxidation is important in fire retardancy. The reactivity of chars to oxidation is normally higher than pure graphite and a function of the degree of graphitisation. Clay enhanced nanocomposites appears to have better resistance to char oxidation. Currently the char structure formed by clay/polymer nanocomposites is still not clear and is being studied further in our laboratory.

## References

1. Iijima S. Helical microtubules of graphitic carbon. *Nature* 1991;354:56-8.
2. Shaffer MSP, Windle AH. Fabrication and characterization of carbon nanotube/poly (vinyl alcohol) Composites. *Advanced Materials* 1999;11:937-41.
3. Thostenson ET, Ren Z, Chou TW. Advances in the science and technology of carbon nanotubes and their composites: a review. *Compos Sci Technol* 2001;61:1899-1912.
4. Thostenson ET, Chou T. Aligned multi-walled carbon nanotube-reinforced composites: processing and mechanical characterization, *Journal of Physics D: Applied Physics* 2002;35:L77-L80.
5. Lau KT, Hui D. The revolutionary creation of new advanced materials – carbon nanotube composites. *Composites B* 2002;33:263-277.
6. Kearns JC, Shambaugh RL. Polypropylene fibers reinforced with carbon nanotubes. *Journal of Applied Polymer Science* 2002;86:2079-2084.
7. Miyagawa H, Drzal LT. Thermo-physical and impact properties of epoxy nanocomposites reinforced by single-wall carbon nanotubes, *Polymer* 2004;45:5163-5170.
8. Beyer G. Carbon nanotubes as flame retardants for polymers, *Fire and Materials* 2002;26:291-293.
9. Kashiwagi T, Grulke E, Hilding J, Harris R, Award W, Douglas J. Thermal degradation and flammability properties of poly(propylene)/carbon nanotube composites, *Macromolecular Rapid Communications* 2002;23:761-765.
10. Kashiwagi T, Grulke E, Hilding J, Groth K, Harris R, Butler K, Shields J, Kharchenko S, Douglas J. Thermal and flammability properties of polypropylene/carbon nanotube nanocomposites, *Polymer* 2004;45:4227-4239.
11. Biscoe J, Warren BE. An x-ray study of carbon black, *J. Appl. Phys* 1942;13:364-371.
12. Franklin RE. Crystallite growth in graphitizing and non-graphitizing carbons, *Proc. Roy. Soc.*, 1951;A209:196-218.
13. Franklin RE. The structure of graphitic carbons, *Acta Crystallographica* 1951;4:253-261.
14. Gilman JW, Kashiwagi T, Lichtenhan JD, Nanocomposites: a revolutionary new flame retardant approach, *SAMPE Journal* 1997;33:40-46.
15. Kashiwagi T, Harris RH Jr, Zhang X, Briber RM, Cipriano BH, Raghavan SR, Awad WH, Shields JR, Flame retardant mechanism of polyamide 6-clay nanocomposites, *Polymer* 2004;45:881-891.

## Figure Captions

Fig.1 The relationship between the rate of heat release rate and burning time for EVA and EVA composites containing 5phr multi-walled carbon nanotubes, 5 phr organoclay and the combination of 2.5phr nanotubes and 2.5phr clay respectively. The data was obtained using cone calorimetry under  $35\text{kW/m}^2$  heat flux.

Fig.2 The morphology of the chars produced from clay/EVA, clay/MWNT/EVA and MWNT/EVA nanocomposites following the cone calorimeter test (top row) and the natural burning (bottom row).

Fig.3 The morphology of the chars produced from clay/EVA, clay/MWNT/EVA and MWNT/EVA nanocomposites following the burning at  $600^\circ\text{C}$  for 20 minutes.

Fig.4 The XRD patterns of the three composites before and after burning in the Muffle furnace at  $600^\circ\text{C}$  for 4 minutes.

Fig.5 SEM micrographs of the fractured surfaces of the chars produced from the clay/EVA and MWNT/EVA composites following the burning at  $600^\circ\text{C}$  for 4 minutes.

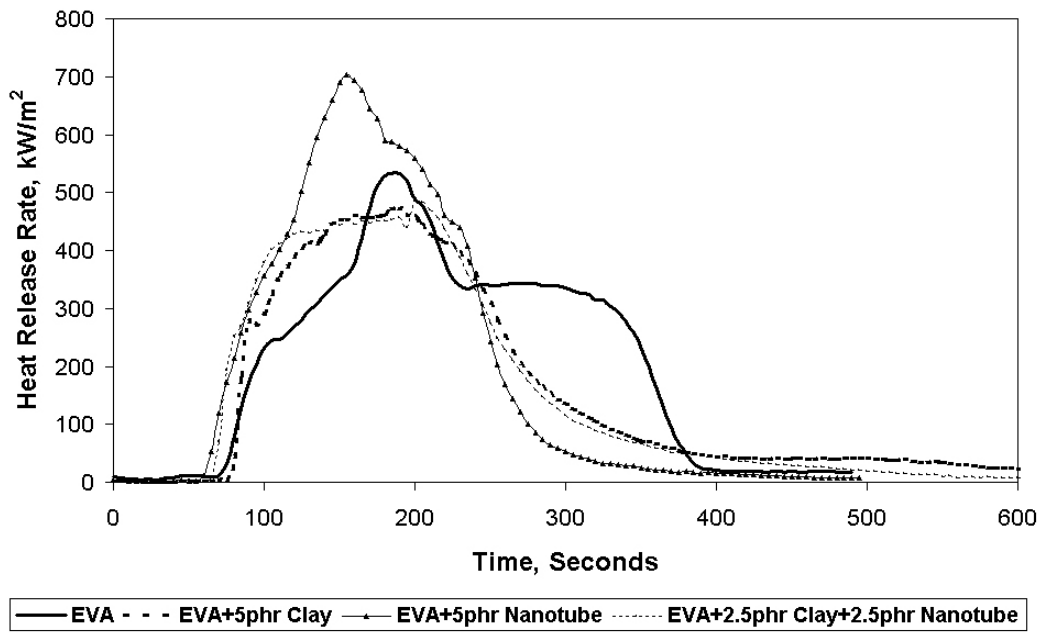


Fig.1 The relationship between the rate of heat release rate and burning time for EVA and EVA composites containing 5phr multi-walled carbon nanotubes, 5 phr organoclay and the combination of 2.5phr nanotubes and 2.5phr clay respectively. The data was obtained using cone calorimetry under  $35\text{kW/m}^2$  heat flux.

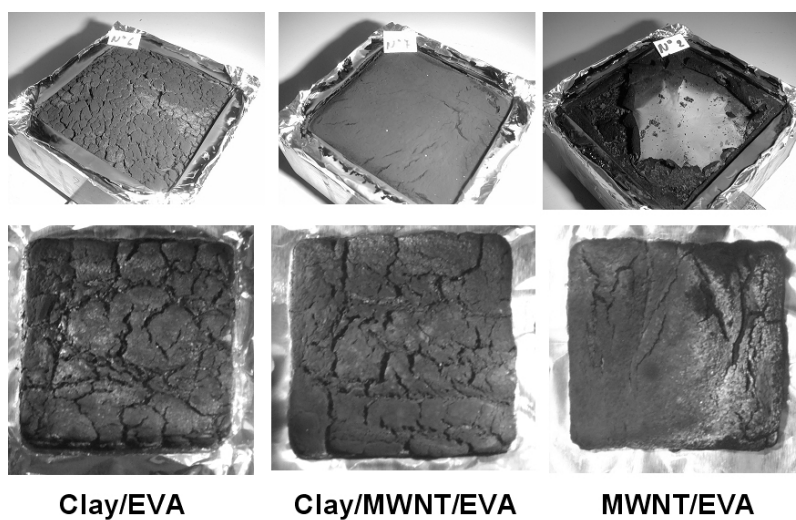


Fig.2 The morphology of the chars produced from clay/EVA, clay/MWNT/EVA and MWNT/EVA nanocomposites following the cone calorimeter test (top row) and the natural burning (bottom row).

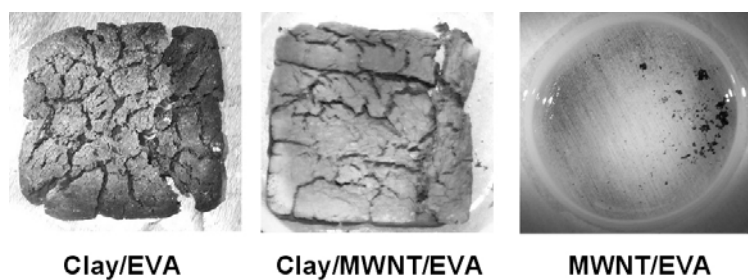


Fig.3 The morphology of the chars produced from clay/EVA, clay/MWNT/EVA and MWNT/EVA nanocomposites following the burning at 600°C for 20 minutes.

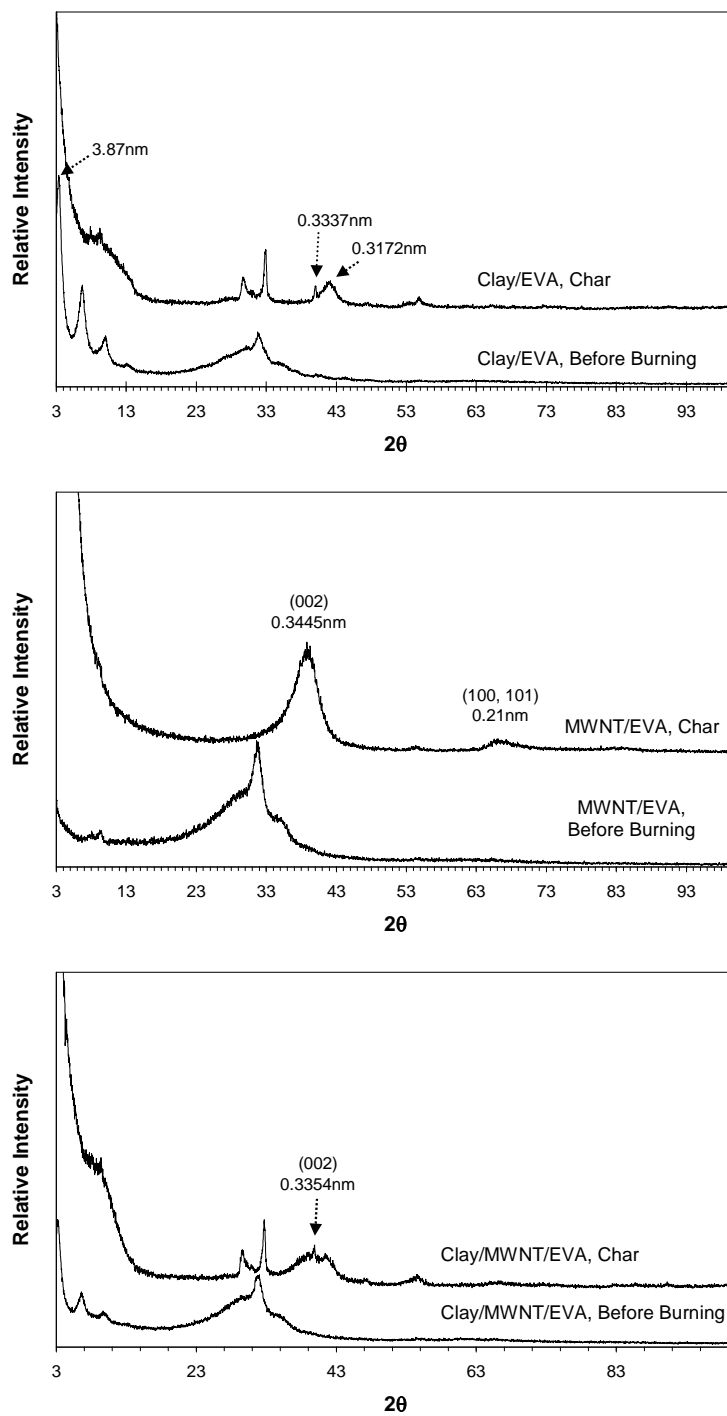
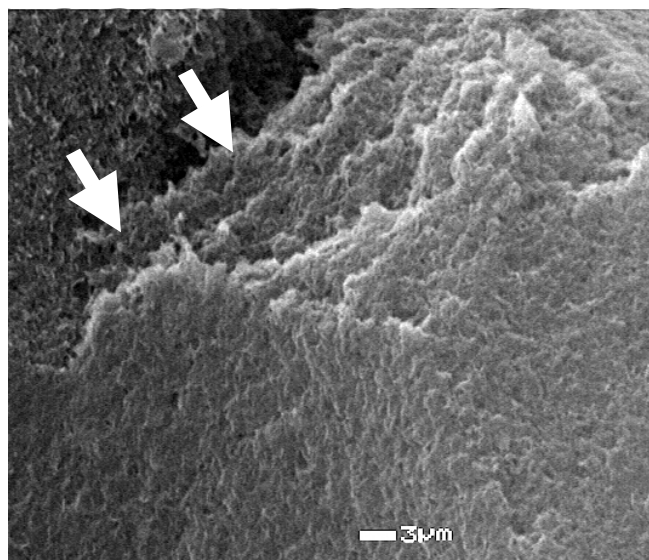
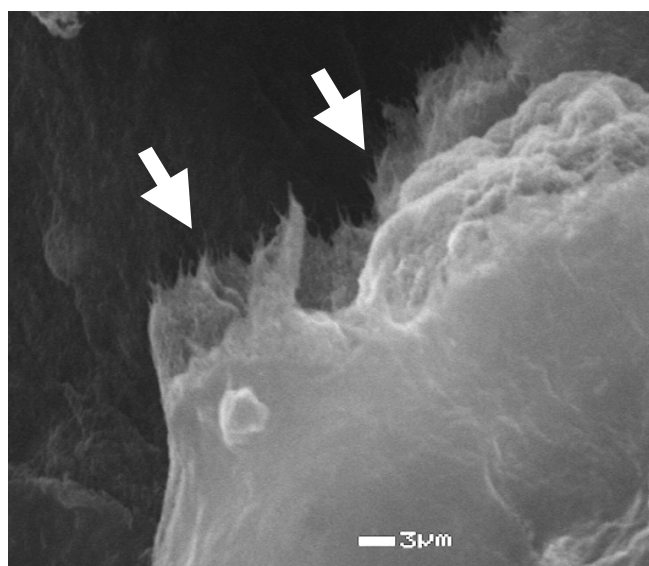


Fig.4 The XRD patterns of the three composites before and after burning in the Muffle furnace at 600°C for 4 minutes.



a) Clay/EVA



b) MWNT/EVA

Fig. 5 SEM micrographs of the fractured surfaces of the chars produced from the clay/EVA and MWNT/EVA composites following the burning at 600°C for 4 minutes.